Separation Science and Technology

Publication details, including instructions for authors and subscription information:
http://www.informaworld.com/smpp/title~content=t713708471

Adsorption Equilibria, Kinetics, and Column Dynamics of Chlorophenols on a Nonionic Polymeric Sorbent, XAD-1600

J. W. Lee[a]; W. G. Shim[b]; J. Y. Ko[b]; H. Moon[b]
[a] Department of Chemical Engineering, Seonam University, Namwon, Korea [b] Faculty of Applied Chemistry, Chonnam National University, Gwangju, Korea

To cite this Article Lee, J. W. , Shim, W. G. , Ko, J. Y. and Moon, H.(2005) 'Adsorption Equilibria, Kinetics, and Column Dynamics of Chlorophenols on a Nonionic Polymeric Sorbent, XAD-1600', Separation Science and Technology, 39: 9, 2041 — 2065

To link to this Article: DOI: 10.1081/SS-120034190

URL: http://dx.doi.org/10.1081/SS-120034190

SEPARATION SCIENCE AND TECHNOLOGY
Vol. 39, No. 9, pp. 2041–2065, 2004

Adsorption Equilibria, Kinetics, and Column Dynamics of Chlorophenols on a Nonionic Polymeric Sorbent, XAD-1600

J. W. Lee,[1] W. G. Shim,[2] J. Y. Ko,[2] and H. Moon[2],*

[1]Department of Chemical Engineering, Seonam University,
Namwon, Korea
[2]Faculty of Applied Chemistry, Chonnam National University,
Gwangju, Korea

ABSTRACT

Adsorption equilibrium, kinetics, and column dynamics of chlorophenols [2-chlorophenol (2-CP) and 2,4-dichlorophenol (2,4-DCP)] dissolved in water were studied using a hydrophobic resin, XAD-1600, without ion-exchange functional groups. In addition, a hydrophilic nonionic polymer resin, XAD-7, and an activated carbon, F400, were chosen for comparative analysis. Adsorption equilibrium data were correlated with the well-known Langmuir, Freundlich, and Sips isotherms. The adsorption amount was in the order of F400 $>$ XAD-1600 $>$ XAD-7. Desorption from polymeric resins adsorbed with chlorophenols was conducted by using two organic solvents [methanol and isopropyl alcohol (IPA)] as desorbates.

---

*Correspondence: H. Moon, Faculty of Applied Chemistry, Chonnam National University, Gwangju 500-757, Korea; Fax: +82-62-530-1899; E-mail: hmoon@chonnam.ac.kr.

DOI: 10.1081/SS-120034190
0149-6395 (Print); 1520-5754 (Online)

www.dekker.com

The intraparticle diffusion mechanism was assumed to be the surface diffusion or pore diffusion. It was found that the diffusivity in desorption step was considerably slower than the diffusivity in adsorption step within polymeric resins. To confirm the possibility of the resin as a sorbent for the removal of chlorophenols, adsorption breakthrough curves were measured under key operating conditions, such as concentration, flow rate, and column length. A simple dynamic model was also formulated to describe both the adsorption and desorption breakthrough curves of chlorophenols.

Key Words: Adsorption; Desorption; Kinetics; Dynamics; Polymeric sorbent.

INTRODUCTION

Chlorophenols are the most common organic pollutants of wastewater. Their sources in the environment are wastewaters from herbicide, pesticide, paint, solvent, petrochemical refinery coal conversion industries, pharmaceutical, pulp, and paper industries.[1] Chlorophenols can be produced also when chlorination is used to disinfect water.[2] Almost all the chlorinated phenols are highly toxic. Thus, the removal or destruction becomes a major environmental concern. To overcome this problem, some removal methods, such as biological treatment, solvent extraction, adsorption, and catalytic oxidation have been used.[3–13] Among them, adsorption is an established and powerful technique for the removal of effluent pollutants.

In recent years, nonionic polymer resins have attracted much attention as an alternative to activated carbon for the removal of organic pollutants for wastewater[8–13] and for the separation of biochemicals.[14–19] Many researchers have been mainly focusing on the adsorption equilibria. In a previous report, Ku and Lee[12] addressed the effect of the presence of functional groups on the benzene ring of various phenols [2-chlorophenol (2-CP), 2,4-dichlorophenol (2,4-DCP), 2,4,6-trichlorophenol, 2-nitrophenol, 2,4-dinitrophenol, 2-methylphenol, and 2,4-dimethylphenol] from aqueous solution by XAD-4 resin. Rexwinkel et al.[20] reported on the adsorption equilibrium of halogenated hydrocarbons (1,1,1-trichloroethane, 1,1,2-trichloroethane, trichloroethene, *trans*-1,2-dichloroethene, chloroform, 2,4,-DCP, and dichloromethane) by wetted and nonwetted hydrophobic XAD-4 and hydrophilic XAD-7 sorbents to investigate the effect of the hydrophobicity of sorbent and sorbate. Also, Juang and Shiau[13] suggested a new, hybrid isotherm to correlate adsorption equilibrium data of phenols on XAD-4 and XAD-7. Although, the polymer resins have lower adsorption capacity for most organics than activated carbon, as they can selectively remove low-molecular-weight organics. Especially, the wide variations in functionality, surface area, and porosity of the resins enable a number of applications for the selective removal of target materials. Unlike the activated carbon, polymeric adsorbents generally have uniform surface chemistry; and they can be synthesized with a controlled pore structure.[14] Such uniformity of properties reduces adsorption heterogeneity and allows regeneration under milder conditions. The regeneration of the resins can be easily accomplished with solvent. The feasibility of an adsorption process depends greatly on the cost of regenerating spent adsorbents. It is well-known that a high temperature and steam is needed for regeneration of spent activated carbons.[4] Although the adsorption capacity of synthetic polymeric sorbents is generally less than that of carbon, these sorbents are advantageous for certain application because their regeneration is easy. In general, there are many regeneration techniques, such as thermal, steam, acid, base, and solvent regenerations.[4,9,13] The choice of a certain regeneration method will depend on the physical and chemical characteristics of both the adsorbate and the adsorbent. For nonionic polymeric adsorbents, the solvent regeneration technique is known to be superior to other methods since the attractive forces binding the adsorbate to the resin surface are physical in nature.[13] In the case of chlorophenols adsorbed on polymeric sorbents, organic solvents are an effective desorbate.[13]

Many researchers previously studied the adsorption rate of benzaldehyde, phenol, dichlorophenol, nitrophenol, and biochemicals in a number of hydrophilic or hydrophobic polymeric adsorbents, such as XAD-2, XAD-4, XAD-7, XAD-8, and XAD-16.[15] Unfortunately, however, nothing has been reported on the adsorption of phenols on XAD-1600. For an efficient removal of chlorophenols dissolved in water, it is essential to understand the adsorption properties including equilibrium, kinetics, and column dynamics. So far, adsorption equilibrium parameters and mass transfer parameters of chlorophenols on XAD-1600 are not available in the published research results. In the present study, therefore, we focused on the acquisition of accurate information on adsorption equilibrium and kinetic data to quantitatively analyze the adsorption and desorption properties of chlorophenols on hydrophobic resin, XAD-1600, as well as hydrophilic resin, XAD-7, to compare the different hydrophobicity of two resins. Desorption can be considered a competitive adsorption between chlorophenols and desorbates. Here, we employed the ideal adsorbed solution theory (IAST)[21] to describe multicomponent equilibria of adsorbate and desorbate on the polymer resin based on the Sips isotherm as a pure component isotherm.[22] A simple, dynamic adsorption model was also formulated by incorporating the IAST with the mass balance equation in the column. The adsorption and desorption breakthrough curves were compared with the simulated results predicted by the model.

THEORY

Adsorption Dynamic Model Based on Surface Diffusion

The dynamic model for adsorption of chlorophenols in the fixed-bed charged with a nonionic polymeric sorbent was formulated according to the following general assumptions:

- The system is isothermal.
- The shape of resin particles is spherical.
- The column is homogeneously packed.
- The pore-size distribution is homogeneous.
- The pore structure inside particles is uniform.
- The fluid physical properties remain constant.
- The flow pattern is a plug flow with a constant linear velocity along the column.
- The surface diffusivities within the adsorbent do not vary.

Under these assumptions, the transport equation inside a spherical adsorbent particle can be described by the following equation:

$$\frac{\partial q_i}{\partial t} = D_{\mathrm{s}i}\left(\frac{\partial^2 q_i}{\partial r^2} + \frac{2}{r}\frac{\partial q_i}{\partial r}\right) \tag{1}$$

with initial and boundary conditions:

$$q_i = q_i(0,\ r) \tag{2}$$

$$D_{\mathrm{s}i}\rho_{\mathrm{p}}\left.\frac{\partial q_i}{\partial r}\right|_{r=R} = k_{\mathrm{f}}(C_i - C_{\mathrm{s}i}) \tag{3}$$

$$\left.\frac{\partial q_i}{\partial r}\right|_{r=0} = 0 \tag{4}$$

The mass balance equation in the column and the relevant initial and boundary conditions are:

$$\frac{\partial C_i}{\partial t} = D_{\mathrm{L}}\frac{\partial^2 C_i}{\partial z^2} - v\frac{\partial C_i}{\partial z} - \frac{1-\varepsilon_{\mathrm{b}}}{\varepsilon_{\mathrm{b}}}\frac{3k_{\mathrm{f}}}{R}(C_i - C_{\mathrm{s}i}) \tag{5}$$

$$C_i = C_i(0, z) \tag{6}$$

$$D_{\mathrm{L}}\left.\frac{\partial C_i}{\partial z}\right|_{z=0} = -v\Big(C_i|_{z=0} - C_{\mathrm{f}i}(t)\big|_{z=0}\Big) \tag{7}$$

$$\left.\frac{\partial C_i}{\partial z}\right|_{z=L} = 0 \tag{8}$$

Adsorption Isotherm

The surface concentration in Eqs. (3) and (5) can be determined from the corresponding adsorption equilibria. Here, we employed IAST as a multicomponent equilibrium theory. A great advantage of IAST is that it requires only single-species isotherm data to predict multicomponent adsorption equilibrium data. To complete the model formulation for the fixed-bed, it is assumed that equilibrium is maintained at the adsorbent particle surfaces; namely C_{si} and q_{si} with $i = 1, 2, \ldots, N$ and $q_{si} = q_i$ at $r = R$ are related by IAST. Once the spreading pressure in IAST is evaluated at a given condition, it completes the adsorption calculation. Here, we omitted the calculation procedure for IAST since the detailed descriptions are found elsewhere.[18,21,23,24]

Numerical Methods

The numerical solutions of the governing equations and boundary conditions were reported previously.[16–18,25] In this study, an orthogonal collocation on finite elements method was used to discretize the first- and second-partial spatial derivatives in both the axial and radial directions. Once the partial differential equations were converted to a system of ordinary differential equations with respect to time, a time integrator, LSODI of the International Mathematics and Science Library, was used to integrate in the time domain.

EXPERIMENTAL

Adsorbates and Adsorbents

The polymeric adsorbents used in this study were XAD-7 and XAD-1600. The former is hydrophilic and a porous aliphatic matrix resin consisting of cross-linked polymethacrylates. The latter is hydrophobic and a spherical polystyrene resin cross-linked with divinylbenzene. They were supplied by Rohm and Haas Co. (USA). Coconut-based activated carbon, F400, was purchased from Cargon Co. (USA). The physical properties of XAD-7, XAD-1600, and F400 used in this study are given in Table 1 and the pore networks of two polymer resins are shown in Fig. 1. The water content of fully swollen resin particles was determined from the weight loss of the samples that occurred while drying in a vacuum oven at 383.15 K for 72 hr. The arithmetic average particle diameter was determined by sorting wet resin particles with the aid of an optical microscope. It was about 560 and 400 μm for XAD-7

Table 1. Properties of polymeric sorbents.

Adsorbent	Unit	F400	XAD-7	XAD-1600
Chemical structure	—	Coal-based	Aliphatic, methylacrylate	Aromatic styrene-divinylbenzene
Hydrophobicity		—	Hydrophilic	Hydrophilic
Particle size	μm	840	430–690	350–450
Particle density	m^3/kg	815	760	459
Particle porosity	—	0.56	0.43	0.55
Moisture holding capacity	%	—	67	69
Surface area (BET)	m^2/g	1012	450	840
Average pore diameter	Å	27	51	63
Specific gravity[a]	—	—	1.05	1.04

[a] From the manufacturer's report.

and XAD-1600, respectively. Nitrogen adsorption–desorption was measured on an ASAP 2010 volumetric adsorption apparatus (Micrometrics) at 77.4 K. The surface area was calculated by using the BET method. The pore diameter was obtained from the BJH pore-size distribution method. The average pore diameters of XAD-7 and XAD-1600 are 51 and 63 Å.

Two chlorophenols, including 2-CP and 2,4-DCP, were used for model compounds. They were purchased from Junsei Co. (Japan). The important properties of 2-CP and 2,4-DCP are shown in Table 2. Isopropyl alcohol (IPA) and methanol were supplied by Carlo Erba (USA), and the purity was greater than 99%. These materials were used without further purification.

Equilibrium Experiment

Prior to experiments, the adsorbent was leached with IPA for 24 hr to wet internal pores. Adsorbent particles were loaded in a 0.02-m ID glass column, and a 10 bed-volume of sodium hydroxide (0.1 N) and HCl (0.1 N) were passed through the column successively at a flow rate of $1.0 \times 10^{-4}\,m^3/min$ to remove impurities. Finally, a 20 bed-volume of distilled and deionized water was passed through at the same flow rate to rinse-off HCl. The experiments were carried out by contacting a given amount of adsorbent with adsorbate solution of $1–8\,mol/m^3$ and organic solvent solution of $300–1500\,mol/m^3$ in an incubator shaking at a constant temperature (298.15 K). The dry base weight of the adsorbent was measured after it was dried for 48 hr in a vacuum oven at 383.15 K. After equilibrium was reached, the excess

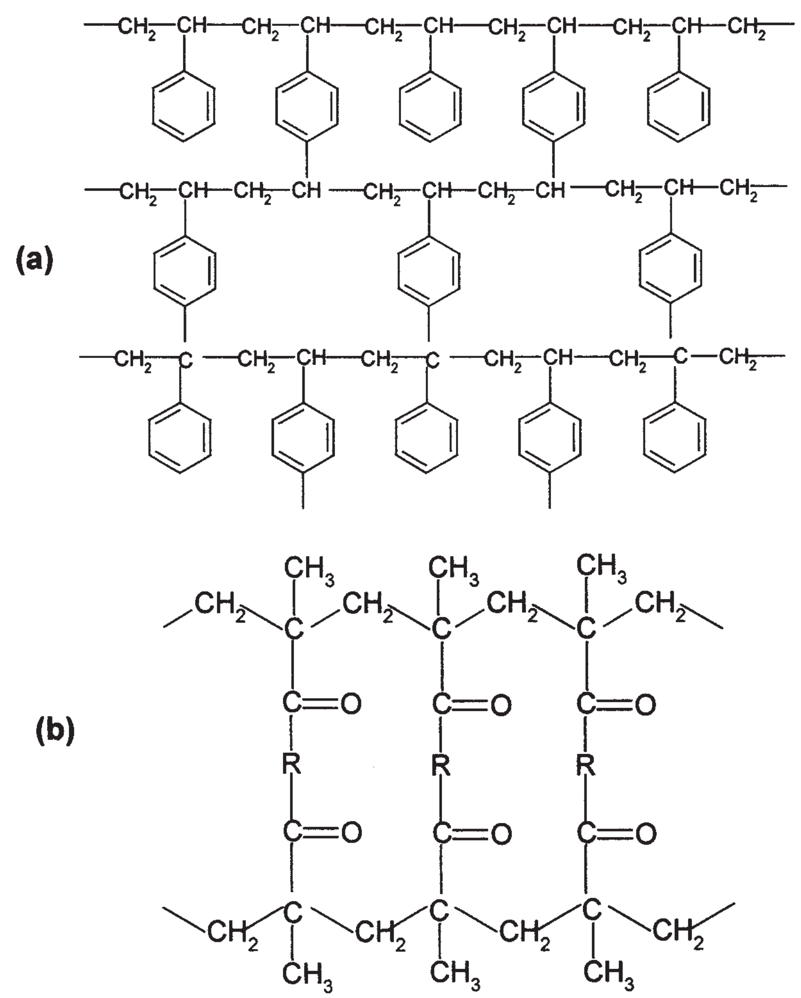

Figure 1. Pore structures of crosslinked polymer resin; (a) polystyrene; (b) polymethacrylate.

2-CP and 2,4-DCP left in solutions were analyzed by using UV spectrometry (Varian, model DMS 100s). The concentrations of IPA and methanol were analyzed by using a gas chromatography (GC) (Shimadzu, model GC14B) equipped with a hydrogen flame ionization detector. Helium was used for a carrier gas. The adsorption capacity of the polymeric adsorbent was determined from material balance.

Table 2. Properties of model compounds used in adsorption studies.

	2-CP	2,4-DCP
Formula	C_6H_5ClOH	$C_6H_3OCl_2OH$
Molecular weight	128.56	163.01
Melting point	43	45
Boiling point	217	210
Vapor pressure	0.10	—
Log(K_{ow})	2.17	3.23
pK	8.55	7.85
Solubility in water (g/100 mL)	2.85	0.45
Specific gravity	1.31	1.38

Batch Experiment

To obtain concentration decay curves, batch experiments were conducted in a carberry-type batch adsorber of $2.0 \times 10^{-3}/m^3$. Sorbent particles were loaded into four cages made of stainless-steel screen. The cages were affixed to the rotating shaft to permit good contact with the solution. All the experiments were carried out at approximately 500 rpm. As in the adsorption experiment, desorption was conducted using organic solvent as a desorbate. The chlorophenol loaded adsorbent was filtered using Whatman filter paper and washed gently with water to remove any unadsorbed sorbates. Then, the adsorbent charged into cages was agitated at 500 rpm for 2 hr with desorbates such as IPA and ethanol and distilled water. The desorbed chlorophenols were analyzed as before.

Fixed-Bed Experiment

The adsorption column was made of glass with an inside diameter of 0.015 m and a length of 0.3 m. A nonionic polymeric sorbent was packed into the column and sustained by glass beads. The solution was introduced upward into the column. To prevent channeling and to enhance the distribution of the solution through the column, two layers of small glass beads were packed in the top and bottom regions of the column. All the packing procedures were conducted under water to avoid the generation of bubbles in the column. After the start of experiments, samples were periodically taken at the determined time intervals by using a fractional collector. The operating conditions of the column are listed in Table 3. Stock solutions were prepared in a glass tank of 5-L volume, and it was placed in a constant-temperature water

Table 3. Experimental conditions for fixed-bed adsorption.

Variables	Units	Values
Particle density	kg/m^3	459
Paticle porosity	—	0.61
Bed length (L)	m	0.05–0.15
Bed diameter (D)	m	0.01
Bed density	kg/m^3	275
Flow rate (ν)	mL/min	4, 6, 8
Temperature	K	298.15
Regenerant (IPA and EtOH)	vol%	10

bath. The flow was controlled at constant rate using a micrometering pump. Distilled water was supplied into the column at the same flow rate as the aqueous solution for about 2 hr prior to the start of experiments to fill the bed with water and to prevent sudden disturbance of the experimental system at the beginning of the experiments. To maintain the column at constant temperature, a water bath with a temperature controller was used. For desorption experiment, IPA and methanol were used as desorbates.

RESULTS AND DISCUSSION

Equilibrium Study

Adsorption isotherms are the most fundamental and informative data on an adsorption system. It is also very important in model prediction for analyzing and designing an adsorption process. Adsorption onto synthetic polymer sorbent is generally driven by the force dispersed between the adsorbate and the resin. Thus, the adsorption capacity depends on the properties of the sorbate and the sorbent. Figure 2 shows the adsorption isotherms of 2-CP and 2,4-DCP on F400, XAD-1600, and XAD-7 at 298.15 K. The adsorption capacity of adsorbents for two chlorophenols decreased in the order F400 > XAD-1600 > XAD-7 on a mass basis. Actually, the adsorption capacity per unit area of XAD-7 is higher than that of XAD-1600 because the specific surface area of XAD-7 ($450\,m^2/g$) is much smaller than XAD-1600 ($840\,m^2/sec$) as listed in Table 1. Similar results were reported by Juang and Shiau.[13] They compared adsorption properties of phenol and 4-chlorophenol on XAD-4 and XAD-7. In contrast to XAD-4, the adsorption amount of phenols on per unit area of XAD-7 is high because of the esterlinkage of the sites for hydrogen bonding provided by XAD-7.

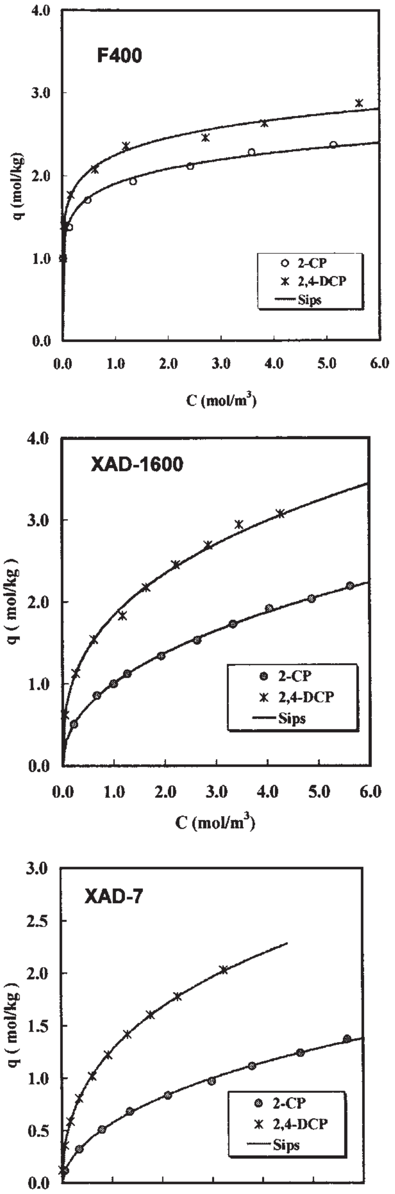

Figure 2. Adsorption isotherms of 2-CP and 2,4-DCP on F400, XAD-1600, and XAD-7 at 298.15 K.

The higher value of $\log(K_{\mathrm{ow}})$ listed in Table 2 means more hydrophobicity. Contrary to our expectation, the adsorption capacity for more hydrophobic 2,4-DCP is always higher on both hydrophilic and hydrophobic polymer resins. Ku and Lee[12] reported a similar result, that is, that the adsorption amount depends on the hydrophobicity of sorbates. They suggested that the adsorption affinity between adsorbent and hydrophobic adsorbate can be linearly correlated with the organic solvent content of the adsorbent. This means that adsorption is relevant to the dispersion and hydrophobic interactions between the nonionic polymeric sorbents and the hydrophobic character of sorbates. Also, according to their report, the presence of functional groups on the benzene ring of various phenols plays an important role on the adsorption amount. The solid lines in Fig. 2 are the predicted results, and the used isotherm parameters of Langmuir, Freundlich, and Sips isotherms are listed in Table 4. Freundlich and Sips isotherms have been found to adequately describe the adsorption of the two chlorophenols. The isotherm parameters were determined by minimizing the mean percentage deviations between experimental and predicted amounts adsorbed based on a modified Levenberg–Marquardt (IMSL routine DUNSLF). The object function, E (%), represents the average percentage deviation between experimental and predicted results as follows:

$$E\,(\%) = \frac{100}{N}\sum_{k=1}^{N}\left[\frac{\left|q_{\mathrm{exp},k} - q_{\mathrm{cal},k}\right|}{q_{\mathrm{exp},k}}\right] \tag{9}$$

The isotherm parameters and the mean percentage deviation error of sorbates on two nonionic polymer resin (XAD-4 and XAD-16) and activated carbon (F400) are listed in Table 5.

From the economic point of view, the success of an adsorption system usually depends on the regeneration of the sorbent. Choice of the desorption method will depend on the physical and chemical characteristics of sorbates and the sorbents. For nonionic polymeric sorbents, the solvent regeneration technique has been considered to be superior to other methods. Grzegorczyk and Carta[14] suggested that desorption of solutes by the addition of organic

Table 4. Single-component adsorption isotherms used.

Name	Model equations	Parameters
Langmuir	$q = (q_m bC)/(1 + bC)$	q_m, b
Freundlich	$q = k_f C^{1/n}$	k_f, n
Sips	$q = (q_m bC^{1/n})/(1 + bC^{1/n})$	q_m, b, n

Table 5. Adsorption isotherm parameters of chlorophenols on sorbents at 298.15 K.

Isotherm type	F400		XAD-7		XAD-1600	
	2-CP	2,4-DCP	2-CP	2,4-DCP	2-CP	2,4-DCP
Langmuir						
q_m	2.400	2.669	1.775	2.158	2.625	3.371
b	32.247	49.902	0.540	2.083	0.664	1.549
E (%)	18.43	23.82	12.85	19.46	8.51	14.76
Freundlich						
k_{f}	2.402	2.709	0.553	1.252	1.005	1.834
n	6.722	7.569	1.897	2.262	2.226	2.817
E (%)	0.91	0.92	2.57	2.02	0.96	1.61
Sips						
q_m	6.785	12.830	5.74	9.730	30.49	114.32
b	0.537	0.265	0.111	0.150	0.034	0.016
n	5.108	6.547	1.707	2.098	2.141	2.779
E (%)	0.40	0.57	0.90	0.39	0.94	1.70

solvents is carried out either by the competitive adsorption of the adsorbate surface or by the effect of the organic solvent on the activity of the solute in the fluid phase. On the other hand, Rivera-Utrilla and colleagues[4] stated that desorption efficiency depends on the accessibility of the organic solvent into the pores, the solubility of the adsorbate in organic solvent, and the adsorbate–adsorbent interactions. In this study, we employed IPA and methanol as desobates and the desorption results in batch and fixed-bed adsorbers are described by using a competitive adsorption model.

Adsorption isotherms of IPA and methanol on XAD-1600 at 298.15 K were measured, and the results are shown in Fig. 3. The amount of IPA adsorbed is much greater than that of methanol. The determined parameters of Langmuir, Freundlich, and Sips isotherms, as well as the mean percentage deviation error, are listed in Table 6. Langmuir and Sips isotherm equations were found to fit the IPA and methanol data well. Determination of these isotherm parameters is required for quantitative prediction of the desorption process, which is assumed to be a competitive adsorption between chlorophenols and organic solvents on nonionic polymeric sorbent. The single-component isotherm parameters of desorbate are required in the calculation of the multicomponent equilibria, namely, IAST, to describe the competitive adsorption between adsorbate and desorbate. Apart from the discussion on exact desorption mechanism, our major concern is first to quantitatively analyze the desorption behavior in a fixed bed for the optimization of cyclic

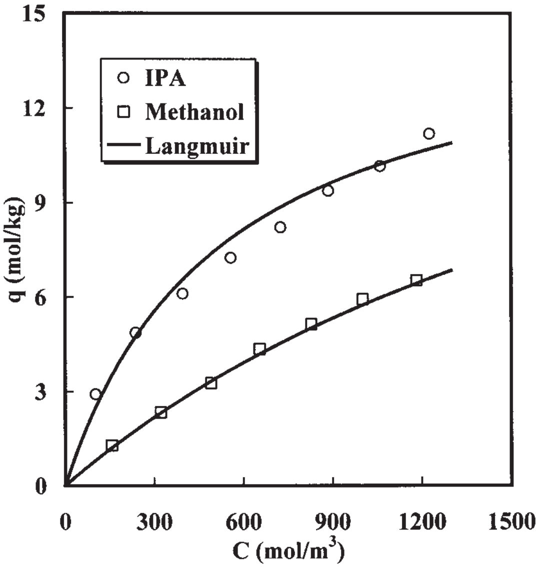

Figure 3. Adsorption isotherms of IPA and MeOH on XAD-1600 at 298.15 K.

Table 6. Adsorption isotherm parameters of IPA and methanol on XAD-1600 at 298.15 K.

Isotherm type	IPA	Methanol
Langmuir		
q_m	15.169	19.041
b	1.9×10^{-3}	4.3×10^{-4}
E (%)	5.796	1.840
Freundlich		
k_f	0.243	0.0206
n	1.875	1.2213
E (%)	1.561	1.6857
Sips		
q_m	252.203	52.21
n	1.0×10^{-3}	3.0×10^{-4}
b	1.8489	1.1453
E (%)	1.533	1.461

operation consisting of adsorption, desorption, and washing. Thus, we assumed that the desorption of adsorbate with the addition of organic solvents is carried out based on the competitive adsorption of the adsorbate and desorbate on a given adsorbent surface.

Kinetic Study

In most of the adsorption processes where highly porous sorbents are used, the external mass-transfer resistance maybe neglected when comparing it with that of intraparticle diffusion. However, it is important to estimate the order of magnitude. In this work, we estimated k_f from the initial concentration history obtained within 300 sec when the diffusional resistance did not significantly prevail.[19] The determined values of k_f are in the range of 0.23 to $1.48 \times 10^{-4}\,\mathrm{m/sec}$ under the experimental conditions listed in Table 7. On the other hand, the determination of intraparticle diffusion coefficients is an important task since intraparticle diffusion is usually the rate-controlling step in most adsorption processes.[23] Intraparticle diffusion within porous sorbents depends on the mechanism of adsorbate transport; namely, pore diffusion, surface diffusion, and others. However, the mechanism of adsorbate transport cannot be completely understood because of its complicated characteristics. To overcome this difficulty, many workers have dealt with a certain major mechanism as a matter of convenience.[7,23,24] In this work, the surface diffusion model (SDM) and the pore diffusion model (PDM) were chosen. Here, we do not mention diffusion model equations and numerical technique to solve equations. Those contents are described in detail in previous articles.[7,18,19] Among various methods for determining the diffusion coefficient, the most general method is to compare the experimental concentration history and the predicted one by using the specified diffusion model.[23,24] Since the diffusion coefficient obtained by this method reflects all kinds of

Table 7. Kinetic parameters in a batch adsorber.

Adsorbents	Adsorbates	$k_f \times 10^4$ (m/sec)	$D_s \times 10^{12}$ (m^2/sec)	$D_p \times 10^9$ (m^2/sec)
F-400	20-CP	1.48	3.91	5.98
	2,4-DCP	1.27	3.00	9.08
XAD-7	2-CP	0.23	8.23	4.39
	2,4-DCP	0.56	2.93	1.55
XAD-1600	2-CP	0.58	17.5	13.4
	2,4-DCP	0.79	10.5	20.3

mass transfer resistance inside a particle, it has been called the effective diffusion coefficient. The experimental concentration decay curves of 2-CP and 2,4-DCP on F400, XAD-7, and XAD-16, were investigated. Similar concentration decay curves can be observed for all sorbents. A typical result for XAD-1600 is shown in Fig. 4 together with the solid lines predicted by using SDM and PDM.

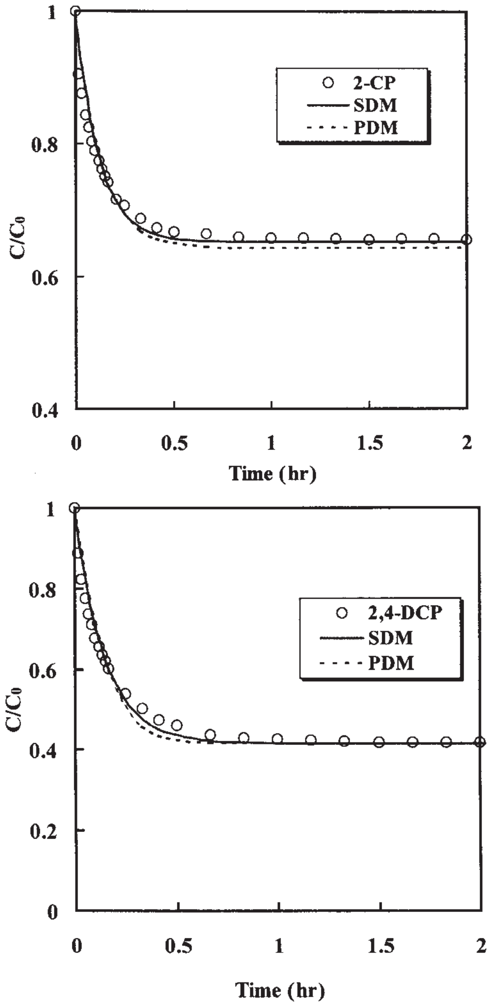

Figure 4. Comparison of diffusion models for experimental concentration decay curves of 2-CP and 2,4-DCP on XAD-1600 batch adsorber ($V = 2\,\text{L}$, $w = 0.99\,\text{g}$, and $C_0 = 1\,\text{mol/m}^3$).

There are no distinct differences according to the diffusion model. The determined effective surface and effective pore diffusion coefficients are in the range of 2.93 to 17.50×10^{-12} and 1.55 to $20.30 \times 10^{-9}\,\mathrm{m^2/sec}$, respectively, as listed in Table 7. As expected, the effective diffusivities of XAD-1600 were one-order-of magnitude greater than those of XAD-7 because of the different pore sizes and surface hydrophobicity of the polymeric sorbents. The pore size of XAD-1600 (63 Å) is slightly greater than that of XAD-7 (51 Å). Similar studies on the adsorption of benzaldehyde on XAD-4 at 298.15 K were reported by Komiyama and Smith.[26] They concluded that the effective pore diffusivity was $1.69 \times 10^{-10}\,\mathrm{m^2/sec}$, and the effective surface diffusivity was $1.10 \times 10^{-12}\,\mathrm{m^2/sec}$. Also, van Vliet et al.[27] reported a surface diffusion coefficient of $2.10 \times 10^{-12}\,\mathrm{m^2/sec}$ for the adsorption of phenol from aqueous solution on XAD-4.

Figure 5 shows the adsorption and desorption uptake curves of 2-CP on XAD-1600 obtained in a batch adsorber. The determined diffusion coefficient for desorption step ($1.29 \times 10^{-14}\,\mathrm{m^2/sec}$) was much slower than that for adsorption step ($1.75 \times 10^{-11}\,\mathrm{m^2/sec}$). Figure 6 shows the experimental and predicted concentration decay curves of 2-CP on XAD-1600 as a function of concentration. The determined effective diffusion coefficients were slightly increased with concentration, and the values are in the range of 1.75 to $3.26 \times 10^{-11}\,\mathrm{m^2/sec}$. In addition, the experimental desorption curves from XAD-1600 adsorbed with 2-CP were obtained as functions of desorbate kinds (IPA, ethanol, and water). As expected, the kinetics of two organic solvents is faster than that of water in polymer resin, XAD-1600. However, it was found that even though pure water without organic solvents was used, 2-CP was desorbed quite well, but it took a slightly longer time. It should be noted that when one uses an organic solvent to regenerate the adsorbent, additional cost is required to separate the mixture of chlorophenol and organic solvent after the regeneration step.

Column Study

The rate of adsorption by porous adsorbents is generally controlled by the transport within the particle, rather than by the intrinsic kinetics of sorption at the surface.[23,24] In this study, the axial dispersion coefficient was determined by using the Wakao and Funazkri equation.[28] The external mass-transfer coefficient in the column was estimated by using the Ranz and Marshall equation.[20] The average axial dispersion coefficient determined under our experimental conditions is $1.5 \times 10^{-6}\,\mathrm{m^2/sec}$, and the external film mass-transfer coefficient is $2.5 \times 10^{-5}\,\mathrm{m^2/sec}$. The intraparticle diffusion coefficient was determined by comparing the experimental concentration decay curves

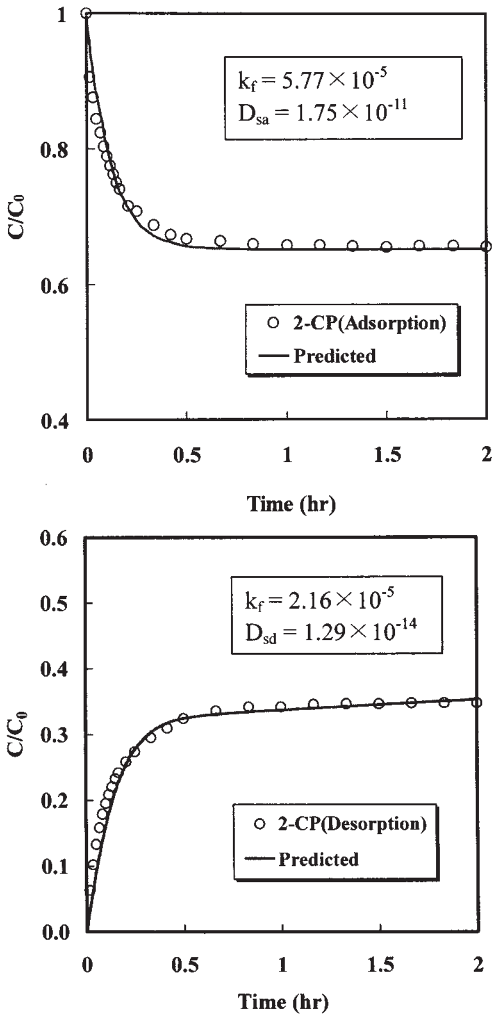

Figure 5. Comprison of mass-transfer resistance in adsorption and desorption steps from the concentration decay and uptake curves of 2-CP on XAD-1600 batch adsorber ($V = 2\,\mathrm{L}$, $w = 0.99\,\mathrm{g}$, and $C_0 = 1\,\mathrm{mol/m^3}$).

obtained in a batch adsorber and the simulated results from a specified diffusion model, for example, PSM or SDM, as described in the previous section.

The breakthrough curve of species in general depends on adsorption equilibrium, interparticle mass transfer, and the hydrodynamic conditions in the column. These factors tend to make the breakthrough curves more dispersive

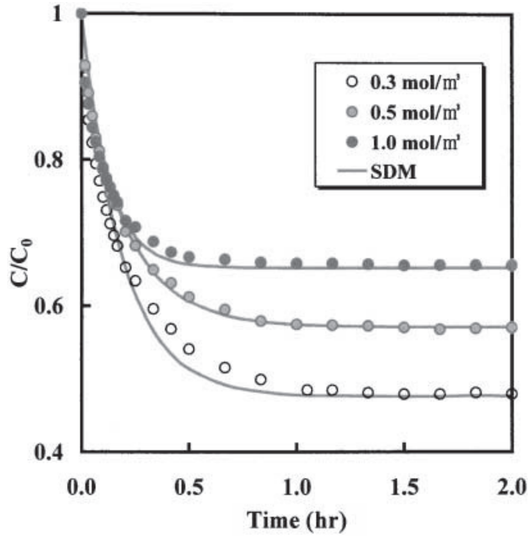

Figure 6. Experimental and predicted decay curves of 2-CP on XAD-1600 as a function of initial adsorbate concentration ($V = 2\,\mathrm{L}$ and $w = 0.87\,\mathrm{g}$).

or less sharp. Therefore, it is reasonable to consider adsorption equilibrium and mass transport simultaneously in simulating the adsorption behavior in the fixed-bed adsorber.[23,24] The operational factors, such as input concentration, flow rate, and column length, are important in column designing and optimization. In this work, breakthrough curves were obtained under the experimental conditions summarized in Table 3, and the corresponding results are shown in Figs. 7 through 9 together with the predicted curves based on the proposed model. The parameters determined in the previous section were used in these calculations without further adjustment.

Figure 7 shows the experimental and predicted adsorption breakthrough curves of pure 2-CP and 2,4-DCP in a XAD-1600 column. The predicted breakthrough curves were obtained using the proposed model. Unlike 2-CP, some deviations between experimental and predicted results for 2,4-DCP can be observed. As expected, the adsorption breakthrough time of 2-CP is faster than that of 2,4-DCP because of the different adsorption affinity to the hydrophilic nonionic polymeric resin, XAD-1600, as shown in Fig. 2. Figure 8 shows the influence of key operating conditions, such as flow rate, column length, and concentration, on adsorption breakthrough curves together with the simulated results. A good agreement between experimental and simulated results can be observed. The shape of breakthrough curves obtained in terms of flow rate and column length is constant, while that in terms of

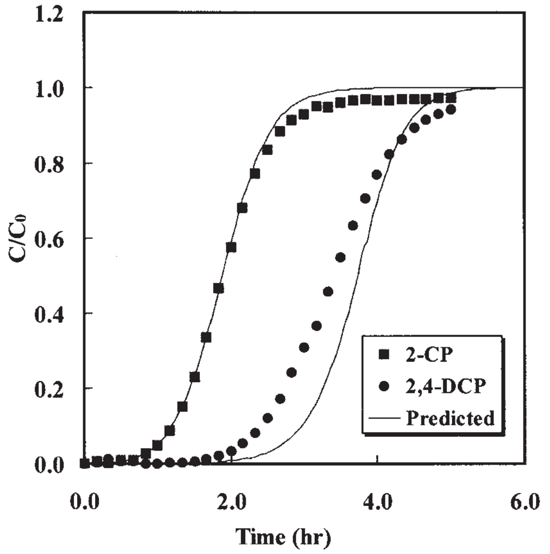

Figure 7. Adsorption breakthrough curves of 2-CP and 2,4-DCP on XAD-1600 at 298.15 K ($C_0 = 1\,\mathrm{mol/m^3}$, $v = 4.23 \times 10^{-3}\,\mathrm{m/sec}$, and $L = 0.1\,\mathrm{m}$).

concentration is steeper. This result can be explained by the concept of the moving velocity of the mass-transfer zone.[17,21,22]

$$V_{\mathrm{MTZ}} = \left(\frac{\partial z}{\partial t}\right)_C = -\frac{(\partial C/\partial t)_z}{(\partial C/\partial z)_t} = \frac{v}{1 + \rho_p((1-\varepsilon_b)/\varepsilon_b)(dq/dC)_c} \tag{10}$$

Mass-transfer zone is a function of interstitial velocity (v), particle density (ρ_p), bed porosity (ε_b), and the gradient of adsorption isotherm, dq/dC. For a linear isotherm adsorption system, the values of dq/dC are constant with other fixed variables. Thus the moving velocity of the MTZ (V_{MTZ}) is constant. The breakthrough time is not affected by input concentrations. However, the adsorption equilibrium of 2-CP on XAD-1600 is nonlinear and favorable isotherm, as shown in Fig. 2. As the input concentration increases, the value of dq/dC decreases so that the zone velocity increases. Therefore, the breakthrough time becomes shorter under this condition. Also, the shape of the breakthrough curve is somewhat steeper at higher input concentration than that at lower input concentration. This may result from larger intraparticle diffusivity because the adsorption zone is reduced by higher diffusion flux.

The solvent regeneration of polymeric adsorbents is particularly effective when the components adsorbed are very soluble in the solvent and the solvating

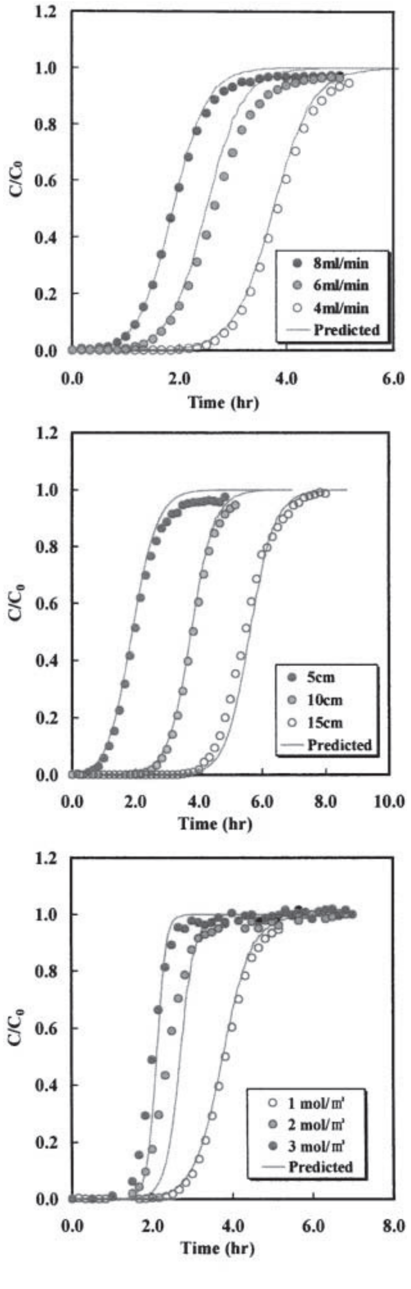

Figure 8. Adsorption breakthrough curves of 2-CP and 2,4-DCP on XAD-1600 at 298.15 K in terms of flow rate, column length, and concentration (reference condition: $C_0 = 1\,\text{mol/m}^3$, $v = 4.23 \times 10^{-3}\,\text{m/sec}$, and $L = 0.1\,\text{m}$).

force is much greater than the physical adsorption force holding the adsorbate onto the resin. Most solvents are adsorbed by polymeric adsorbents. In many cases, they penetrate the gel phase of the polymeric matrix. This results in the solvent displacement of the component adsorbed in the resin. In this study, IPA and methanol were used as regenerants to desorbe chlorophenols from XAD-1600. Figure 9 shows desorption breakthrough curves of 2-CP in XAD-1600 column to check the effect of IPA and methanol on them. When IPA was used as a desorbate, the overshoot in desorption curve became higher, and desorption occured quickly compared with methanol. The high-regeneration efficiency of IPA results from the contribution of solubility and affinity of 2-CP to XAD-1600. So, if the excess amount of IPA does not make any trouble in the process to remove chlorophenols dissolved in water, a higher concentration of IPA maybe used to perform the regeneration step more effectively. However, the optimal condition depends on the economic point of view. Also, the higher concentration of organic solvents can involve a fire risk in industrial plants. The proposed dynamic model based on the competitive adsorption model, IAST, describes desorption breakthrough curves satisfactorily without adjustment of model parameters determined in the previous sections. Some deviations may come from the inaccurate diffusivity

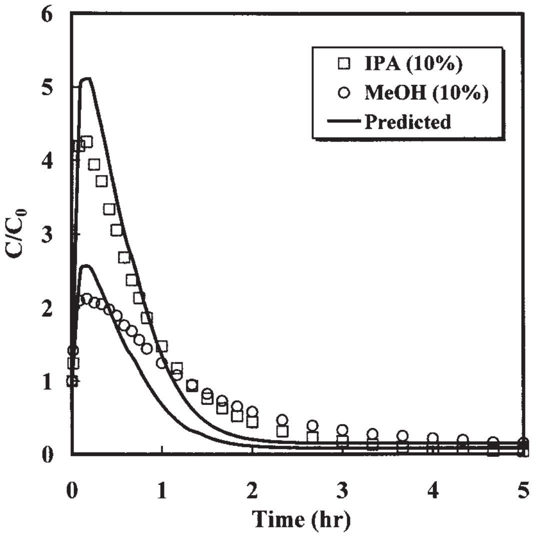

Figure 9. Effect of organic solvents on desorption breakthrough curves in XAD-1600 adsorber saturated with $C_0 = 1\,\mathrm{mol/m^3}$ of 2-CP at 298.15 K ($v = 2.11 \times 10^{-3}\,\mathrm{m/sec}$ and $L = 0.1\,\mathrm{m}$).

determined in batch adsorber. When the lower effective surface diffusivity is used, more precise results can be obtained. Thus, further works on desorption studies are required for the analysis of desorption mechanism and the determination of diffusivity in terms of the water–alcohol mixing ratio.

CONCLUSION

As a removal technology for chlorophenols dissolved in aqueous solution, adsorption equilibrium, kinetics, and column dynamics were investigated in a finite batch adsorber and in a fixed-bed column charged with nonionic polymer resins. Adsorption equilibrium data of two chlorophenols (2-CP and 2,4-DCP) as well as two organic solvents (methanol and IPA) on nonionic polymer resins (XAD-7 and XAD-1600) and activated carbon (F400) correlated well with Sips isotherm. It was found that the adsorption amount of 2,4-DCP was always greater than that of 2-CP on both hydrophilic XAD-7 and hydrophobic XAD-1600 polymer resins. Despite the surface hydrophobicity of polymeric sorbents, adsorption capacity increased with the hydrophobicity of adsorbates. Intraparticle diffusion mechanism was assumed to be the surface diffusion or pore diffusion. The effective diffusion coefficients were determined by comparing experimental and predicted concentration histories obtained in finite batch adsorbers. The determined coefficient in the desorption step was much slower than that in the adsorption step. The desorption of two chlorophenols from resin using IPA and methanol was described reasonably by a competitive adsorption model, IAST, based on the Sips equation as a single-component isotherm. Experimental adsorption and desorption breakthrough curves of 2-CP and 2,4-DCP were simulated by the proposed simple dynamic model successfully. However, further works on desorption mechanism and its exact diffusivity are needed for precise analysis of desorption breakthrough curves. The proposed model in this study can be effectively used in the design, scale-up, and optimization of resin columns for the removal of organic pollutants through a cyclic mode that has three typical steps including adsorption, desorption, and washing.

NOMENCLATURE

b	Langmuir constant (m^3/mol) or Sips constant [$(m^3/mol)^{(1/n)}$]
C	Concentration in the fluid phase (mol/m^3)
C_s	Concentration in equilibrium with the adsorbed phase (mol/m^3)
D_L	Axial dispersion coefficient (m^2/sec)

D_p	Pore diffusion coefficient (m^2/sec)
D_s	Surface diffusion coefficient (m^2/sec)
E	Percentage error (%)
k_f	Film mass-transfer coefficient (m/sec)
k_F	Freundlich constant (mol/kg)
L	Column length (m)
n	Freundlich or Sips constant (−)
N	Number of data points (−)
q	Cconcentration in particle phase (mol/kg)
q_m	Langmuir or Sips constant (mol/kg)
r	Radial distance (m)
R	Particle radius (m)
t	Time (sec)
z	Axial distance (m)

Greek Letters

ε_b	Column porosity (−)
ρ_p	Particle density (kg/m^3)
υ	Interstitial velocity (m/sec)

Superscripts and Subscripts

i	Component
exp	Experimental
cal	Calculated

Abbreviation

CP	Chlorophenol
DCP	Dichlorophenol
IAST	Ideal adsorbed solution theory
IPA	Isopropyl alcohol
MeOH	Methanol
MTZ	Mass-transfer zone

ACKNOWLEDGMENT

This work was partially supported by grant No. R-01-2001-000-00414-0 (2002) from the Korea Science and Engineering Foundation.

REFERENCES

1. Aksu, Z.; Yener, J.A. Comparative adsorption/biosorption study of mono-chlorinated phenols onto various sorbents. Waste Manage. **2001**, *21*, 695–702.
2. Streat, M.; Patrick, J.W.; Camporro-Perez, M.J. Sorption of phenol and *p*-chlorophenol form water using conventional and novel activated carbons. Water Sci. Res. **1995**, *29*, 467–478.
3. Tseng, R.L.; Wu, F.C.; Juang, R.S. Liquid-phase adsorption of dyes and phenols using pinewood-based activated carbons. Carbon **2003**, *41*, 487–495.
4. Rivera-Utrilla, J.; Ferro-Garcia, M.A.; Bautista-Toledo, I.; Sanchez-Jimnenz, C.; Salvador, F.; Merchan, M.D. Regneration of ortho-chlorophenol-exhausted activated carbons with liquid water at high pressure and temperature. Water Res. **2003**, *37*, 1905–1911.
5. Huang, H.H.; Lu, M.C.; Chen, J.N.; Lee, C.T. Catalytic decomposition of hydrogen peroxide and 4-chlorophenol in the presence of modified activated carbons. Chemsphere **2003**, *51*, 935–943.
6. Namasivayam, C.; Kavitha, D. Adsorptive removal of 2-chlorophenol by low-cost coal pith carbon. J. Hazard. Mater. **2003**, *B98*, 257–274.
7. Moon, H.; Lee, W.K. Intraparticle diffusion in liquid-phase adsorption of phenols with activated carbon in finite batch adsorber. J. Coll. Interf. **1983**, *96*, 162–171.
8. Moon, H.; Lee, J.W.; Park, H.C. Adsorption of phenols in a fixed-bed adsorber charged with polymeric sorbents. Korean J. Chem. Eng. **1992**, *9* (4), 25–232.
9. Lee, J.W.; Yang, J.H.; Moon, H. A simple model for regeneration of a polymeric sorbent saturated with phenol. Korean J. Chem. Eng. **1995**, *12* (1), 88–94.
10. Li, A.; Zhang, Q.; Zhang, G.; Chen, J.; Fei, Z.; Liu, F. Adsorption of phenolic compounds from aqueous solutions by a water-compatible hypercrosslinked polymeric adsorbent. Chemsphere **2002**, *47*, 981–989.
11. Li, A.; Zhng, Q.; Chen, J.; Fei, Z.; Long, C.; Li, W. Adsorption of phenolic compounds on amberlite XAD-4 and its acetylated derivative MX-4. React. Funct. Polym. **2001**, *49*, 225–233.
12. Ku, Y.; Lee, K.C. Removal of phenols from aqueous solution by XAD-4 resin. J. Hazard. Mater. **2000**, *B80*, 59–68.
13. Juang, R.S.; Shiau, J.Y. Adsorption isotherms of phenols from water onto macroreticular resins. J. Hazard. Mater. **1999**, *B70*, 171–183.
14. Grzegorczyk, D.S.; Carta, G. Adsorption of amino acids on porous polymeric adsorbents-I. Equilibrium. Chem. Eng. Sci. **1996**, *51* (5), 807–817.

15. Grzegorczyk, D.S.; Carta, G. Adsorption of amino acids on porous polymeric adsorbents-II. Intraparticle mass transfer. Chem. Eng. Sci. **1996**, *51* (5), 819–826.
16. Lee, J.W.; Park, H.C.; Moon, H. Adsorption and desorption of cephalosporin C on nonionic polymeric sorbents. Sep. Purif. Tech. **1997**, *12*, 1–11.
17. Lee, J.W.; Jung, H.J.; Moon, H. Effect of operating conditions on adsorption of cephalosporin C in a column adsorber. Korean J. Chem. Eng. **1997**, *14* (4), 277–284.
18. Lee, J.W.; Moon, H. Effect of pH on adsorption of cephalosporin C by a nonionic polymeric sorbent. Adsorption **1999**, *5*, 381–390.
19. Xie, Y.; Sandt, E.V.D.; Weerd, T.D.; Wang, N.-H.L. Purification of adipoyl-7-amino-3-deaceoxycephalosporanic acid from fermentation broth using stepwise elution with a synergistically adsorbed modulator. J. Chromatogr. **2001**, *908*, 273–291.
20. Rexwinkel, G.; Heesink, B.B.M.; Swaaij, W.P.M. Adsorption of halogenated hydrocarbons from aqueous solutions by wetted and nonwetted hydrophobic and hydrophilic sorbents: equilibria. J. Chem. Eng. Data **1999**, *44*, 1139–1145.
21. Myers, A.L.; Prausnitz, J.M. Thermodynamics of mixed gas adsorption. AIChE J. **1965**, *11*, 121–127.
22. Sips, R. Structure of a catalyst surface. J. Chem. Phys. **1948**, *16*, 490–495.
23. Ruthven, D.M. Thermodynamics of adsorption. In *Principles of Adsorption and Adsorption Processes*; Wiley: New York, 1984; 62–85.
24. Yang, R.T. Adsorbents and adsorption isotherms. In *Gas Separation by Adsorption Processes*; Butterworths: Boston, 1986; 26–48.
25. Villadesen, J.V.; Stewart, W.E. Solution of boundary-value problems by orthogonal collocation. Chem. Eng. Sci. **1967**, *22*, 1483–1501.
26. Komiyama, H.; Smith, J.M. Intraparticle mass transport in liquid filled pores. AIChE J. **1974**, *20*, 728–737.
27. van Vliet, B.M.; Weber, W.J., Jr.; Hozumi, H. Modeling and prediction of specific compound adsorption by activated carbon and synthetic adsorbents. Water Res. **1980**, *14*, 1719–1829.
28. Wakao, N.; Funazkri, T. Effect of fluid dispersion coefficients on particle-to-fluid mass transfer coefficients in packed beds: correlation of Sherwood numbers. Chem. Eng. Sci. **1978**, *33*, 1375–1384.

Received September 2003
Accepted January 2004